

Available online at www.sciencedirect.com

ScienceDirect

journal homepage: www.elsevier.com/locate/ijhydene

Electrodes based on nafion and epoxy-graphene composites for improving the performance and durability of open cathode fuel cells, prepared by electrospray deposition

M.A. Gómez^a, A.J. Navarro^a, J.J. Giner-Casares^b, M. Cano^b,
A.J. Fernández-Romero^a, J.J. López-Cascales^{a,*}

^a Universidad Politécnica de Cartagena, Dep. Ing. Química y Ambiental, Campus Alfonso XIII, Aulario C, Cartagena, 30203, Murcia, Spain

^b Departamento de Química-Física, Universidad de Córdoba, 14014, Córdoba, Spain

HIGHLIGHTS

- The electrospray technique allows the fabrication of nanostructured electrodes for its use in fuel cells.
- The addition of epoxy/graphene to the catalytic ink improves the performance of the fuel cells.
- The presence of epoxy/graphene improves the adherence of the catalyst to the proton membrane.

ARTICLE INFO

Article history:

Received 4 January 2022

Received in revised form

2 February 2022

Accepted 16 February 2022

Available online 10 March 2022

Keywords:

Fuel cell

Epoxy

Electrodes

Graphene

Electrospray

ABSTRACT

Fabrication of electrodes for polymer electrolyte fuel cells is a intriguing process in which a balance between gas transport, electrical conductivity, proton transport and water managing must be optimized. In this work four different electrodes prepared by electrospray deposition have been studied using different catalytic inks, in which Nafion and epoxy doped with Graphene-Nanoplatelets were used as binders. After studying the behavior of those electrodes in a single open cathode fuel cell proton electrolyte membrane, it is clear that the addition of epoxy as binder doped with graphene, improves the performance of the fuel cell and increase the mechanical stability of the electrode avoiding the loose of catalyst during the electrode manipulation in the fuel cell assembly process and the durability of the fuel cell. To explain this behavior, an ex-situ study was carried out, in which properties such as its surface morphology, hydrophobicity and electrical and thermal conductivity of those electrodes were studied. From the results of this study, such improvement in the performance of the fuel cell was justified on the basis of the increase in the electrical conductivity, a diminution in its thermal conductivity and an enhancement of hydrophobicity (surface morphology) of the deposited catalyst layer, when an optimum quantity of epoxy is added to the catalytic ink that makes to improve the mechanical properties of those electrodes.

© 2022 The Author(s). Published by Elsevier Ltd on behalf of Hydrogen Energy Publications LLC. This is an open access article under the CC BY license (<http://creativecommons.org/licenses/by/4.0/>).

* Corresponding author.

E-mail address: javier.lopez@upct.es (J.J. López-Cascales).

<https://doi.org/10.1016/j.ijhydene.2022.02.146>

0360-3199/© 2022 The Author(s). Published by Elsevier Ltd on behalf of Hydrogen Energy Publications LLC. This is an open access article under the CC BY license (<http://creativecommons.org/licenses/by/4.0/>).

Introduction

During the last decades, hydrogen is attracting a great interest as a valuable tool for achieving the decarbonization of our society [1–3]. Proton electrolyte fuel cell is an electrochemical device in which takes place the hydrogen oxidation at the anode and the oxygen (or air) reduction at the cathode. A key component of those fuel cells is the membrane electrode assembly (MEA), which is constituted by the gas diffusion layer (GDL), the catalyst layer (platinum supported on carbon in most of the cases) and the proton membrane. Thus, the interface between the proton membrane and the electrode is a critical part of this MEA due to several aspects that reduces the meanlife of those fuel cells, such as the physical, mechanical and chemical degradation of those electrodes.

An effective electrode must keep a right balance between its electrical conductivity, its permeability to gases and water managing [4–6]. In this context, a key objective that is searched during the electrode preparation is the optimization of the catalyst distribution along the three space dimensions with the aim of maximizing its catalytic activity by favoring the contact between the three neighbor phases: electrolyte, gas and catalyst [7]. In this sense, one possibility is to put directly in contact the catalyst with the membrane (with the objective of diminishing the interface resistances) together with the use of sophisticated deposition techniques that provide certain three dimensional architecture to the catalyst [4].

So far, one typical way to do so is using a catalytic ink with nafion as binder, and to generate the electrode directly in contact with the proton membrane. Lee et al. [8] investigated the effect of nafion impregnation of the catalytic ink on the performance of PEMFC electrodes, obtaining that when oxidant is air, the optimum nafion loading was 0.6 mg/cm^2 , but if this quantity is increased, the performance dropped very sharply.

Hence, the catalytic layers are designed for generating high rates of the desired reaction with the minimum quantity of catalyst for reaching the required level of power output. To achieve that objective, it is necessary to generate a large interface between the polymer electrolyte and the catalyst, an efficient transport of protons from the anode to the cathode, an easy transport of the reactant gases, an efficient removal of the condensed water, and a continuous electronic current passage from the electrode to the current collector [9]. Hence, the improvement of the catalytic activity is a consequence of the balance of all the above points.

In this context, the electrospray technique [10–14] reached a great notoriety during the last years for generating a tridimensional architecture in the catalyst deposition [15]. In this regard, several works showed that this experimental techniques optimized the quantity of catalyst required for certain power outputs in comparison with other traditional techniques, such as aerography or paint brush deposition [5,11,16].

Among other types of fuel cells, an open cathode proton exchange membrane fuel cell (OC-PEMFC) is a type of fuel cell in which oxygen is taken from air using an external fan that produces an air convection on the cathode [17–19]. The main advantage of this type of fuel cell compared with the standard

ones with the cathode closes, is that they avoid the use of expensive peripheral devices that introduces severe penalties in their performance. However, it is also true that due to the fact that the cathode is open to air, i. e, air is introduced into the fuel cell at low pressures, water evaporates very rapidly due to its low vapor pressure, heat and air convection, and as a consequence, an increase in the proton membrane resistance is expected [19].

Graphene has been employed in several applications with the objective of improving the proton exchange membrane properties in fuel cells and electrolyzers [20–24]. In this work we propose the reformulation of a new catalytic ink for fabricating the electrodes that are used in an open cathode fuel cells, in which a little quantity of epoxy doped with Graphene-Nanoplatelets (GN) was incorporated as binder to the catalytic ink. The reason why we decided to incorporate such element to the catalytic ink is because epoxy presents a good chemical stability in acid and basic environments, good mechanical properties, and provides certain hydrophobicity that diminish the risk of water flooding in the electrodes [25]. On the other side of the coin, epoxy presents the disadvantage of being an electrical insulator. To overcome this fact, cheap Graphene Nanoplatelets (GN) is added to the epoxy to improve the electrical conductivity of the final composite [26,27].

Experimental

Electrodes preparation

To explore the effect of adding a certain quantity of epoxy to the catalytic ink, four different catalytic inks were generated for the electrode preparation, such as follows:

Ink-1: 0.32 g of 60% Platinum on graphitized carbon (provided by Sigma), and 2.29 ml of Nafion solution (Alfa Aesar, 5 wt %) (which represents 33% of the catalyst weight), in 129 ml of 2-isopropanol (Panreac).

Ink-2: 0.32 g of 60% Pt/C supported catalyst, 2.29 ml of Nafion solution (Alfa Aesar, 5 wt %) (which represents 33% of the catalyst weight), and 60 ppm of graphene nanoplatelets (GN), in 129 ml of 2-isopropanol (Panreac).

Ink-3: 0.32 g of 60% Pt/C supported catalyst, 2.29 ml of Nafion solution (Alfa Aesar, 5 wt %) (which represents 33% of the catalyst weight), 0.05 ml of commercial bicomponent epoxy-polyamide in water solution, and 60 ppm of graphene nanoplatelets (GN), in 129 ml of 2-isopropanol (Panreac).

Ink-4: 0.32 g of 60% Pt/C supported catalyst, 2.29 ml of Nafion solution (Alfa Aesar, 5 wt %) (which represents 33% of the catalyst weight), 0.1 ml of commercial bicomponent epoxy polyamide in water solution, and 60 ppm of graphene nanoplatelets (GN), in 129 ml of 2-isopropanol (Panreac).

The mother ink considered as the starting point for our study was the proposed by Litster et al. [4] based on the use of only Nafion as binder in the catalytic ink. The amount of graphene employed in our catalytic inks responded to the minimum quantity needed to provide a certain electrical conductivity to an initially non-conductive epoxy layer. The

60ppm of graphene nanoplatelets was maintained constant, once an increase up to twice the original quantity was not translated into any improvement of the electrical response of the fuel cell. The graphene nanoplatelets (GN) were provided by Graphite-Shop (www.graphite-shop.com), and were used in their original form. The four solutions were ultrasonicated for 1 h and stirred for 24 h before use.

When the catalytic inks were ready for their use, the electrodes were generated by electrospray deposition of a thin catalytic layer on the proton membrane, till reaching a surface concentration of 0.2 mgPt/cm^2 on the anode and 0.6 mgPt/cm^2 on the cathode.

Electrospray deposition is an experimental technique for transferring particles in the gas phase at atmospheric conditions. Fig. 1 shows the scheme of the electrospray equipment that was developed in our laboratory.

Thus, the injection of a solution in a high electric field leads to an aerosol of charged species which can be deposited on a determined substrate with nanometric dimensions. This technique presents certain advantages respect to others, for example the aerography, because this is a cheap technique that can work at atmospheric conditions, this can generate thin uniform surfaces, and this technique allows to control of the nanometric size of the aerosol charged droplets. During this deposition process, the proton membrane was placed on a warm bed with a digital control of temperature that was fixed at 50° Celsius . To generate the electrospray, 9 kV were applied between the nozzle and the warm bed with a distance of separation of 40 mm, and a nitrogen caudal of 0.1 ml/min at 0.5 bars was required to maintain steady the electrospray jet-cone shape. Fig. 2. a shows the typical cone-jet shape generated during the electrospray deposition. The needle used for producing the electrospray was a standard G-29. The nanoparticles were deposited homogeneously on the surface. Note the ordered arrangement and the absence of multilayers and aggregates of nanoparticles, confirming the convenience of the electrospray method. The nanoparticles displayed an average size of ca. 5 nm.

Nafion NR-212 (DuPont) was the proton membrane employed for testing the electrodes without any pretreatment. eCoCell-BW40-a (Hydrogreen Energy, hydrogreenergy.com)

was the gas diffusion layer used for the MEA preparation. No hot-press was employed in the MEA preparation.

A single open cathode proton exchange membrane (OC-PEMFC) [19,28] was the fuel cell used for testing the electrodes. We chosen this type of fuel cell because closed-cathode PEMFCs require a suite of components such as compressors, pumps, coolant loops, conductive bipolar plates, and humidifiers that suppose a severe penalty to the power output generated by the fuel cell stack. The active area of the electrodes was 23.2 cm^2 . At the cathode side, there was an air convection forced by an external fan, which was controlled electronically as a function of the current demand with the objective of avoiding the dryness of the membrane. Cathode and anode were fabricated in 316-stainless steel with a golden bath, with parallel channels of 2 mm width and ribs of 1 mm width, such as it was described elsewhere [29]. Fig. 3 shows a picture of the single fuel cell used in our study.

The equipment for measuring the electrical conductivity was a FFP5000 four point probe, of Veeco Instruments Inc, and the equipment for measuring the thermal conductivity was homemade. A BK-Precision BA6010 miniOhmmeter at 1 kHz was used for measuring the internal resistance of the single fuel cell. The polarization curves were generated using an electronic DC Load 3721A of Array Electronic Co., Ltd. (<http://www.array.sh/>)

Samples for transmission electron microscopy (TEM) were prepared by depositing under ambient conditions a dispersion of the particles generated by the electrospray on 200 mesh copper grids coated with Formvar/carbon films. TEM images were obtained using a JEOL JEM 1400 TEM microscope, operated at an accelerating voltage of 80 kV.

Results and discussion

Polarization curves

Fig. 4 shows the polarization and power curves of the electrodes generated with the inks introduced above.

The above figure shows as the addition of epoxy to the ink provides a positive contribution to the performance of the fuel

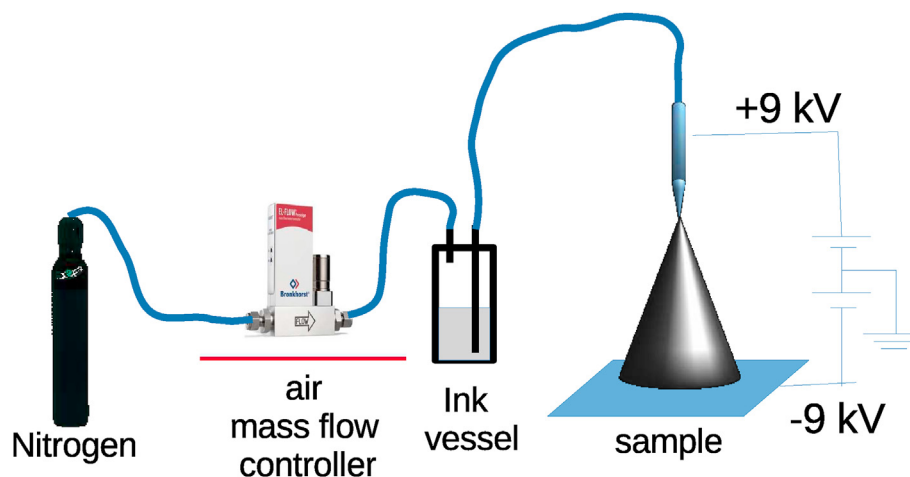


Fig. 1 – Scheme of the installation developed in our laboratory for the electrospray deposition.

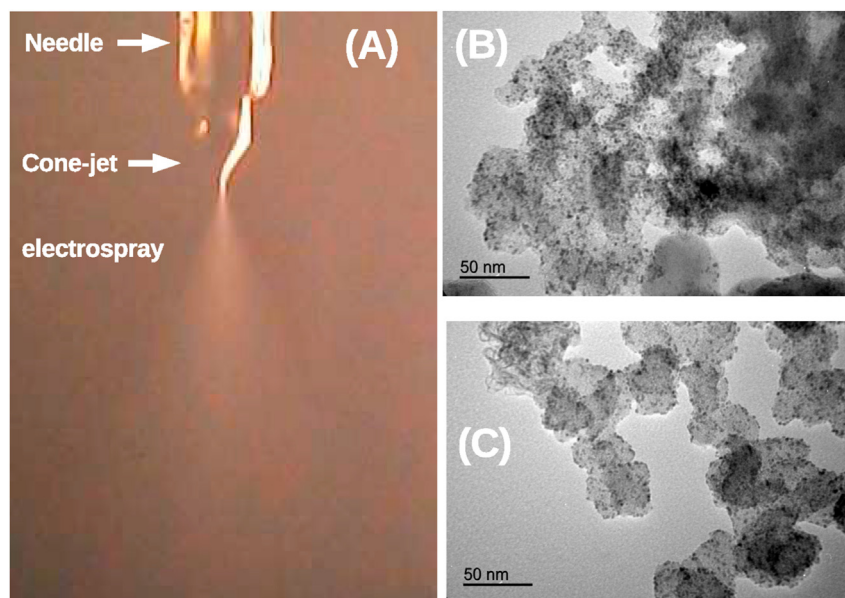


Fig. 2 – (A) Jet shape generated during the electrospay deposition. (B) TEM image after 1 min of ink depositions with the ink-1. (C) TEM images after 1 min of deposition using the ink-3 containing nafion and epoxy in its formulation as binder.

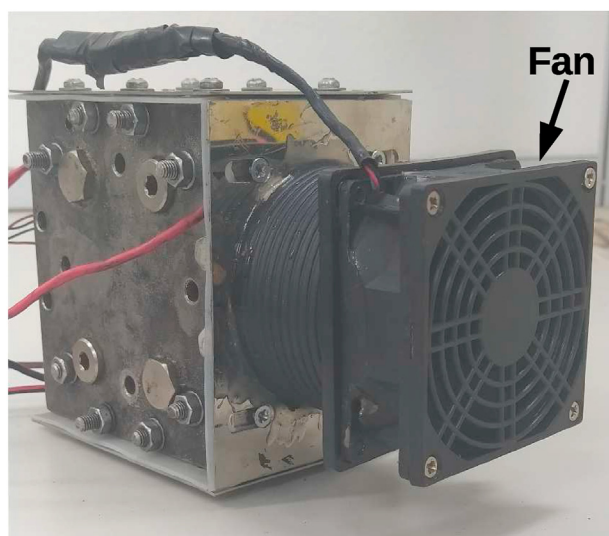


Fig. 3 – Photography of the single open cathode cell (OC-PEMFC) designed in our laboratory for this study.

cell. However, an excess of this binder (Ink-4) produces a diminishing in the potential at open circuit, E_0 , such as it is shown in Table 1. This diminishing in E_0 is clearly associated with an excess of the catalyst impregnation, and as a consequence, an increasing in the electrode overpotential is expected. However, for the ink-3 in which the quantity of epoxy was reduced, this effect disappeared.

To get some insight into the performance of those electrodes, the polarization curves were fit to the empirical equation proposed by Kim et al. [30], such as follows:

$$E = E_0 - b \log i - R \cdot i \quad (1)$$

$$E_0 = E_r - b \log i_0 \quad (2)$$

where, being E_r the reversible potential, i_0 the electrode exchange current, b the Tafel's slope and R the ohmic resistance that gather the contribution of the proton membrane and hardware ohmic resistance.

In this regard, Table 1 shows the fitting parameters of the four polarization curves at different temperatures, considering equation (1). Ink-2 and ink-3 show almost the same values for their Ohmic resistance, which is clearly associated to the presence of graphene in their composition that reduces the ohmic resistance of the electrodes. This behavior contrasts with the found for the electrodes fabricated with the ink-4 in which due to the high epoxy content, their ohmic resistance increased due to the poor electrical conductivity of this binder that is not compensated by the presence of graphene in the blend. It is of special relevance the fact that the electrodes fabricated using inks 1 and 4, their Ohmic resistance increased very much when temperature reached 50° Celsius, in comparison with the electrodes fabricated with the inks 2 and 3, in which graphene was present in their composition.

Table 2 shows the average internal resistance obtained during the generation of the polarization curves. Table 2 shows a good semi-quantitative agreement with the values of Table 1 obtained from fitting the polarization curves using the empirical equation (1). Thus, in general, we see how the internal resistance is maximum for the electrodes generated with ink-1, giving an idea of the poor hydration of the membrane when only nafion is used as a binder. This difference in behavior becomes more noticeable with increasing temperature. Thus, for electrodes made with inks 3 and 4 (both with epoxy in their formulations), lower resistances were obtained than with ink-1 and ink-2, behavior that may be associated with their higher hydrophobicity, such as this will be discussed below.

With the aim of exploring the stability of the electrodes prepared, a test was carried out in a single fuel cell for 1 week,

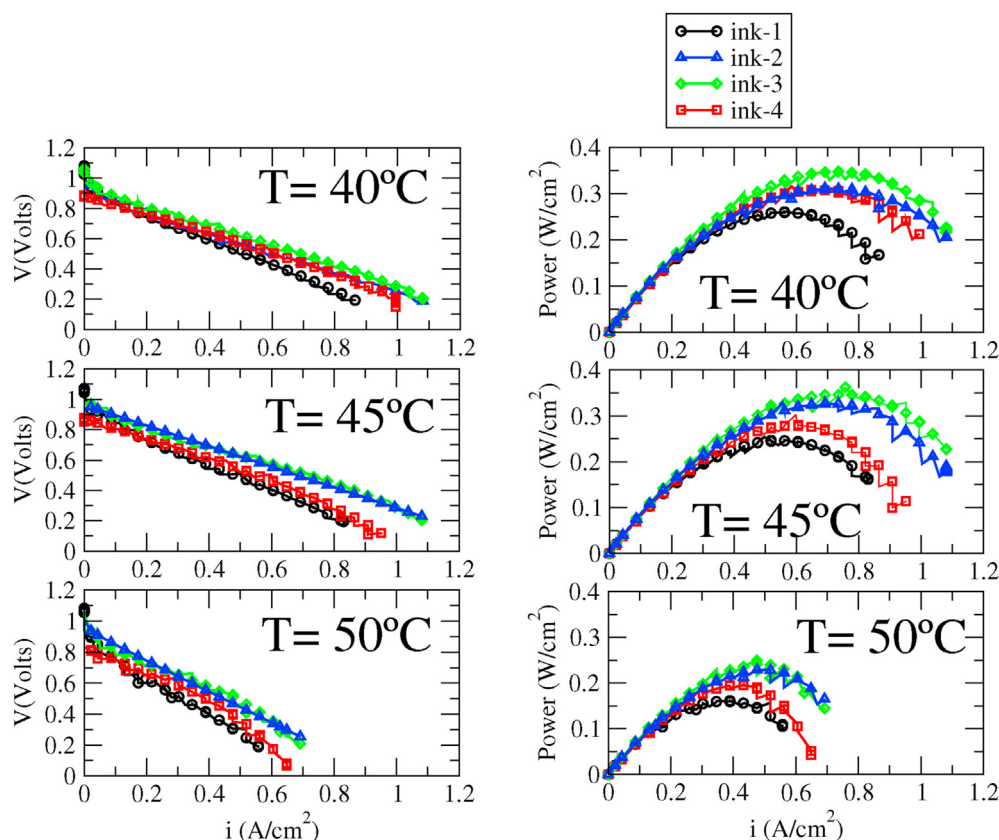


Fig. 4 – Polarization curves corresponding to the electrodes generated using the four inks described in the text, at different temperatures. Solid line shows the fit using equation 1.

Table 1 – Experimental open circuit potential E_0^{exp} and fitting parameters of the polarization curves of Fig. 4, considering the empirical equation (1) proposed by Kim et al. [30], corresponding to the electrodes fabricated with the four catalytic inks described in the text.

Electrode	E_0^{exp} (V)	E_0 (V)	$b(V.dec^{-1})$	R ($\Omega.cm^2$)
T = 40°C				
Ink-1	1.08	0.887	0.0422	0.801
Ink-2	1.01	0.858	0.0543	0.610
Ink-3	1.06	0.931	0.0262	0.652
Ink-4	0.88	0.891	0.00003	0.671
T = 45°C				
Ink-1	1.071	0.871	0.043	0.8126
Ink-2	0.948	0.964	0.00012	0.679
Ink-3	0.964	0.962	0.00009	0.679
Ink-4	0.852	0.880	0.00007	0.729
T = 50°C				
Ink-1	1.08	0.816	0.058	1.135
Ink-2	1.071	0.842	0.046	0.829
Ink-3	1.067	0.928	0.018	0.918
Ink-4	0.834	0.878	0.000025	1.085

Table 2 – Internal resistance measured during the polarization curve generation for the four electrodes studied in this work.

Electrode	$\Omega.cm^2$ (40 °C)	$\Omega.cm^2$ (45 °C)	$\Omega.cm^2$ (50 °C)
Ink-1	0.254	0.414	0.844
Ink-2	0.223	0.262	0.781
Ink-3	0.231	0.274	0.570
Ink-4	0.274	0.347	0.686

working at a steady current density of 0.4 A/cm² for the electrodes prepared with the inks 1, 2, and 3 (electrode prepared with the ink-4 was discarded from this study due to its high internal resistance). Fig. 5 shows the polarization curves after 48 and 168 h working.

Fig. 5 shows how the electrodes generated with ink-1 in absence of graphene and epoxy, were the electrodes that

suffered the major degradation after 1 week (or 168 h). From those results, we deduce that graphene stabilize the structure of the electrode, although the presence of epoxy at low concentrations, improves their stability. From our point of view, two are the facts that justify the benefices of adding epoxy to the catalytic inks: 1. The presence of epoxy together with graphene increases the electrical conductivity of the electrodes because the presence of this binding facilitates the contact between adjacent carbon particles in the catalytic layer and 2. The presence of epoxy as binder increases the hydrophobicity of the electrodes that reduces the flooding effects that degrades the electrodes, such as we will show below.

Electrode morphology

Fig. 2 shows the TEM images after 1 min of deposition for the inks 1 and 3. In this case, we observe different morphology of

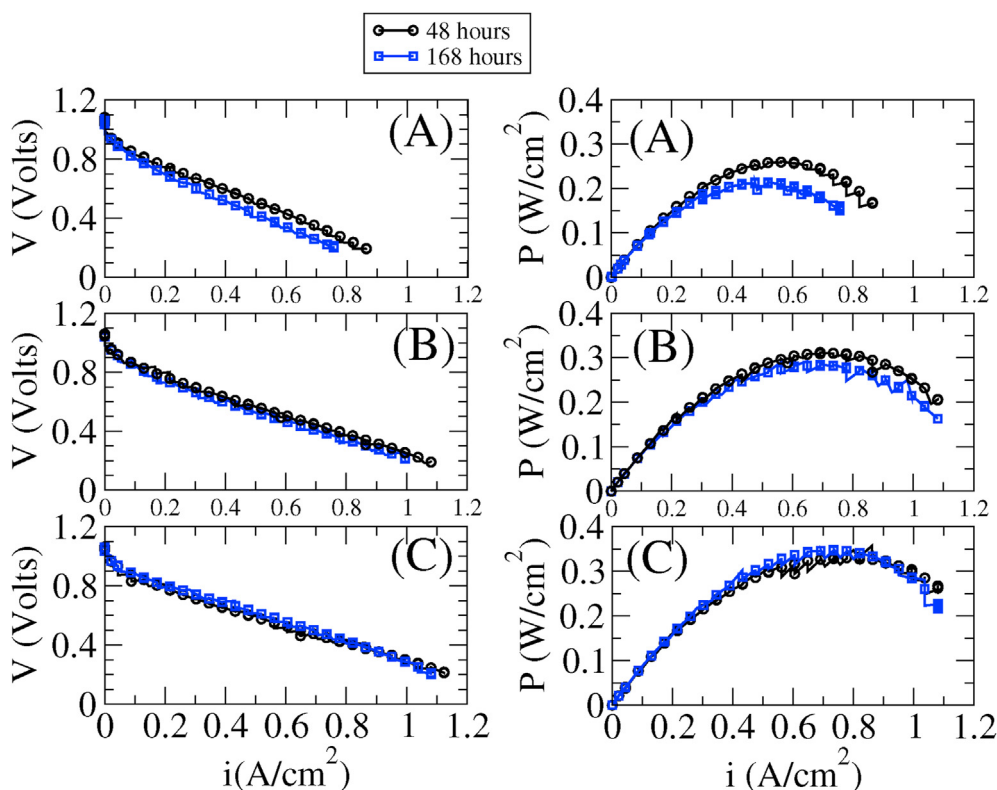


Fig. 5 – Polarization and power curves of the electrodes fabricated with ink-1 (A), ink-2 (B) and ink-3 (C), after working for 48 and 168 h, at a controlled temperature of cathode and anode of 40° Celsius.

the catalyst deposition depending of the type of ink used in their preparation. This difference is expected that can be translated to different architectures of the electrodes generated. Thus, in presence of epoxy, more discrete depositions of roughly 5 nm of diameter are observed in comparison with the case in which only nafion is present as binder.

Fig. 6 shows the images of the four electrodes generated in this work. Those images show an evident change in their morphology that is associated with the type of ink that was used in their preparation. Thus, the electrode fabricated with ink-3 and ink-4 show a rough surface (specially for ink-3) that contrast with the surface of the electrodes generated in the absence of epoxy (inks 1 and 2), in which some slits are observed on their surface. This roughness of the electrode generated with the ink-3 is attenuated when the epoxy content increased (ink-4). This presence of defaults in the surface of the electrodes 1 and 2, maybe the factor that produces the weakness of their mechanical properties. Thus, electrodes prepared with inks 3 and 4 did not peel off during their manipulation (avoiding by the way the loose of catalyst), in comparison with the electrodes generated with the inks 1 and 2 where a certain quantity of catalyst was partially lost after each manipulation. Furthermore, this fact contributed to avoid the loose of catalyst during the long hours of working on the fuel cell, fact that explain the steady fuel cell performance when those electrodes were used in the MEA preparation, in comparison with the electrodes in which the inks 1 and 2 were used in their preparation, where a diminution in their

polarization and power curves is seen after 168 h of working. In general, Fig. 6 shows that the size of the aggregates are between 74 in the absence of epoxy and 67 nm in the presence of epoxy. This diminution in the size of the aggregates could explain the high hydrophobicity of those electrodes in comparison with those electrodes generated in the absence of epoxy, on the basis that hydrophobicity and porosity are two properties that are narrowly associated each other, such as we will discuss below.

The way about how the electrodes manage the water generated during the redox processes inside the fuel cell is an important aspect that affects to the fuel cell performance. In this context, an optimization in the proton membrane hydration is crucial for an optimum performance of the fuel cell [4,31]. Hence in this sense, it seems that the hydrophobicity of the electrodes together with their porosity (properties that are related each other in a certain way [32]) are two critical properties for managing the water generated inside the fuel cell [33].

Fig. 7 shows the contact angle between a water droplet of 30 μL and the surface of the two electrodes generated using the inks 1 and 3.

Such as it was expected, the different surface morphology of the two electrodes is translated to a different hydrophobicity on those electrodes. This difference becomes evident from the contact angles of 110 and 140° of two water droplets with the surface of both electrodes, giving an idea of the increase of hydrophobicity with the presence of epoxy in the catalytic ink.

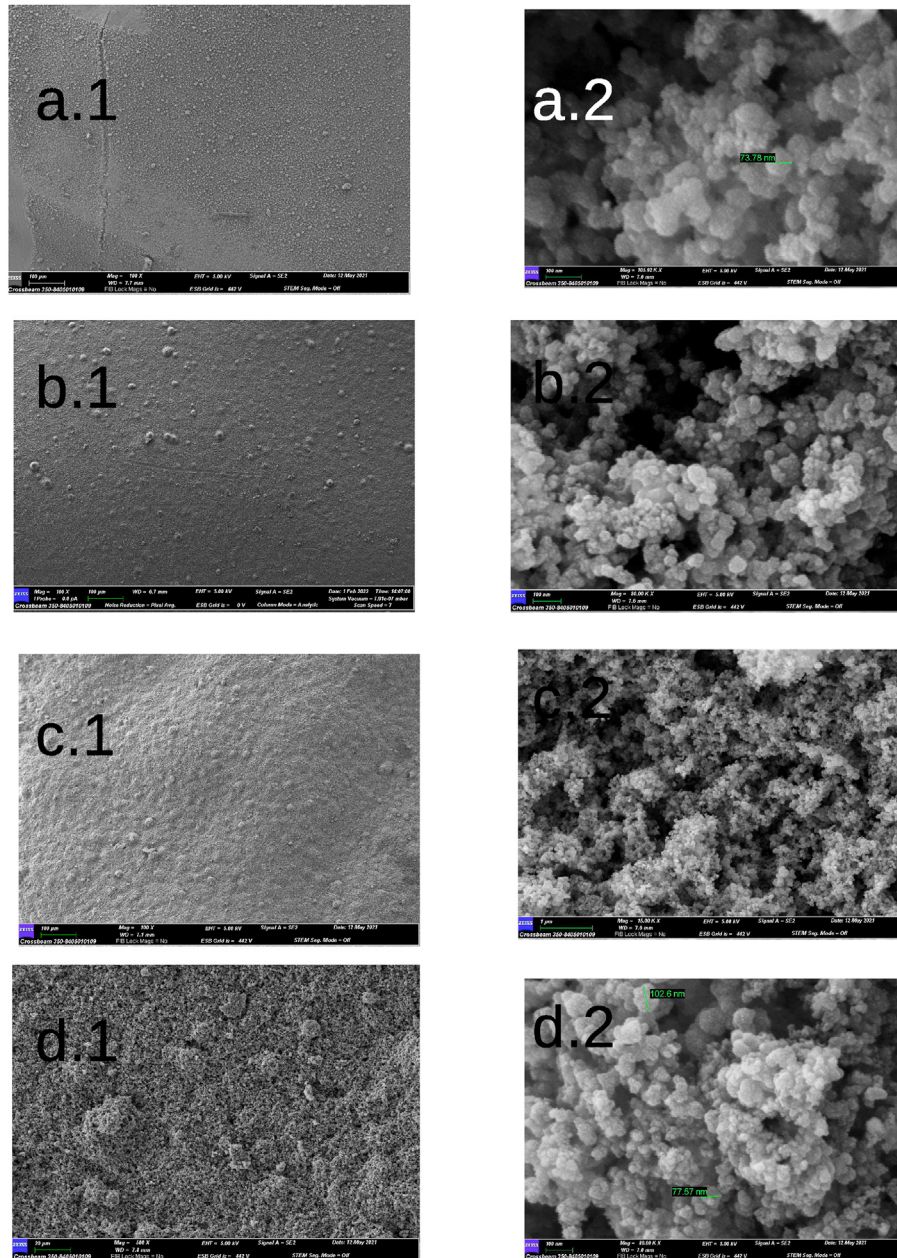


Fig. 6 – SEM images of the four electrodes studied in this work, prepared with the four catalytic inks (a ink 1, b ink 2, c ink 3 and d ink 4) with 100x, and 105000x magnifications, respectively.

Electrical and thermal conductivity

The electrical conductivity was measured using the linear four points method. This technique consisted in measuring the electric potential between two points due to the application of an electrical current between the other two points [34,35]. Hence, the electrical resistivity can be determined as follows [34]:

$$\rho = \frac{\pi t}{\ln 2} \frac{V}{I} \quad (3)$$

where t is the sample thickness, I , the electrical current applied between two points, and V the difference of potential

measured between the other two points. Hence, the electrical conductivity σ in S/m, can be obtained as,

$$\sigma = \frac{1}{\rho} \quad (4)$$

Thus, an electrical conductivity of 48, 187 and 197 S/m was determined for the three electrodes generated with the inks 1, 2, 3 and 4, such as it was described above. From these results, it is clear that the presence of graphene increases in three folds its electrical conductivity, in comparison with the electrode in which only the catalyst was present in the ink. Furthermore, the use of epoxy as binder (ink-3) increased the electrical conductivity respect to the electrode in which only

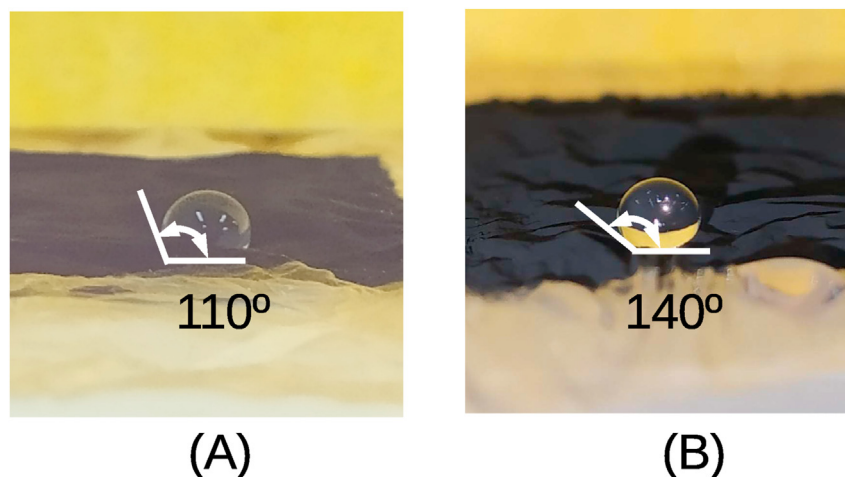


Fig. 7 – Contact angle of a water droplet of 30 μL with the surface of both electrodes generated with the inks 1 and 3, containing nafion and nafion+epoxy as binder in their composition, respectively.

nafion doped with graphene (ink-2) was used as binder. This result can be associated to the special morphology observed in the TEM and SEM images, in which the presence of epoxy contributed to increase the electrical contacts between neighbor particles, increasing by this way its electrical conductivity.

Concerning the thermal conductivity, κ , it can be measured on the assumption that a thin and flat surface divides two isolated environments at different temperature. Keeping this in mind, κ can be measured as follows:

$$\kappa = \frac{b \cdot (T_2^s - T_2^f) \cdot h}{(T_1^s - T_2^s)} \quad (5)$$

where the thermal conductivity κ is attained from the air temperature inside of an isolated chamber T_1^f , the room temperature T_2^f , the temperature on the inlet face of the sample T_1^s , the temperature on the outlet face of the sample T_2^s and the sample thickness, b . In equation (5), h is a parameter that has to be fit using a reference material of known thermal conductivity [29]. After the respective validation of the method,

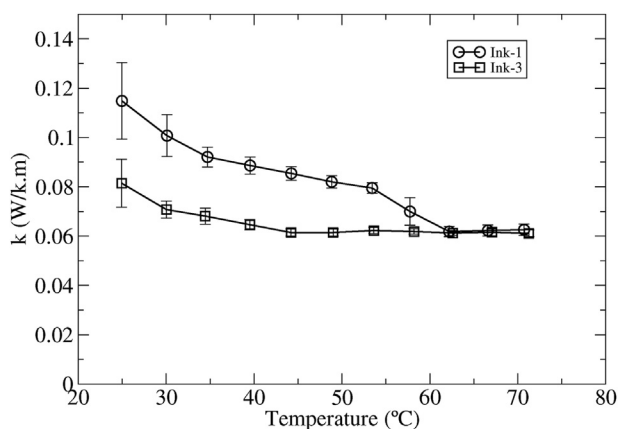


Fig. 8 – Thermal conductivity through plane of the two electrodes studied in this work, fabricated with the inks 1 and 3.

the thermal conductivity through the plane of the two electrodes was determined. Thus, Fig. 8 shows the variation of the thermal conductivity with the temperature for the electrodes generated using the inks 1 and 3.

Fig. 8 shows as the thermal conductivity is much higher for the electrode with only nafion (ink-1) as binder than for the electrode generated using nafion+epoxy doped with graphene (ink-3) for the range from 25 to 65° Celsius. For temperatures above 65°, both electrodes converge to the same thermal conductivity. Owejan et al. [36] suggested that a thermal conductivity below 0.3 $\frac{\text{W}}{\text{K.m}}$ gets less saturated water at high current densities and maintain the oxygen transport resistance at lower levels. In this sense, from our results, it seems that electrodes with lower thermal conductivity improves the performance of the electrodes in the fuel cell because reduce the water condensation at the electrode.

Conclusions

Electrodes are a critical part at the heart of a fuel cell, where its chemical and mechanical stability is crucial for its duration and stability. In this context, a new polymer blend was studied in which epoxy-polyamide doped with cheap Graphene-Nanoplatelets was incorporated to the formulation of the inks used for the preparation of the electrodes. In this context, it was investigated as the presence of epoxy doped with graphene improved the adhesion of the catalyst to the proton membrane, and how the morphology of the electrodes changed when epoxy was incorporated to the catalytic ink formulation. In this context, we showed how the addition of a water soluble epoxy-polyamide to the catalytic ink increased the surface homogeneity of the electrodes generated by electro-spray deposition, and how the presence of epoxy reduced drastically the apparition of slits on the surface of those electrodes, avoiding the peel off effects during the different manipulations of the MEA preparation. Thus, we showed how the coating provided by the electro-spray method was quite homogeneous, fact that was confirmed by transmission electron microscopy measurements.

Furthermore, the use of epoxy as binder enhanced the electrical conductivity of those electrodes, its hydrophobicity, performance, stability and durability. Thus, the improvement of all those properties was reflected into an improvement in the performance of the fuel cell, for the whole range of temperatures studied.

Declaration of competing interest

The authors declare that they have no known competing financial interests or personal relationships that could have appeared to influence the work reported in this paper.

Acknowledgments

AJN and MAG are actually working on this project with a contract funded by the Comunidad Autónoma de la Región de Murcia, Conserjería de Desarrollo Económico, Turismo y Empleo, and the European Union, through the program RIS3-MUR, grant number 2I20SAE00079. This work has also been funded by the Spanish Ministry of Science and Innovation (AEI, Spain, PID2020-112744GB-I00/AEI/10.13039/501100011033 and RTI2018-095844-B-I00), Fundación Seneca (Región de Murcia, Spain), grant number: 20985/PI/18 and Agencia estatal española de Investigación, grant number PID2019-104272RB-C55/AEI/10.13039/501100011033.

REFERENCES

- [1] Busby RL. *Hydrogen and fuel cells*. Pennwell Publishing; 2005.
- [2] Zhang S, Yuan X, Wang H, Merida W, Zhu H, Shen J, Wu S, Zhang J. A review of accelerated stress tests of mea durability in pem fuel cells. *Int J Hydrogen Energy* 2009;34:388–404. <https://doi.org/10.1016/j.ijhydene.2008.10.012>.
- [3] López-Cascales J, Juan-Segovia M, Ibañez-Molina J, Sanchez-Vera J, Vivo-Vivo P. Environmental impact associated with the substitution of internal combustion vehicles by fuel cell vehicles refueled with hydrogen generated by electrolysis using the power grid. an estimation focused on the autonomous region of murcia (Spain). *Renew Energy* 2015;77:79–85. <https://doi.org/10.1016/j.renene.2014.11.082>.
- [4] Litster S, McLean G. Pem fuel cell electrodes. *J Power Sources* 2004;120:61–76. <https://doi.org/10.1016/j.jpowsour.2003.12.055>.
- [5] Fernandez R, Ferreira-Aparicio P, Daza L. Pemfc electrode preparation: influence of the solvent composition and evaporation rate on the catalytic layer microstructure. *J Power Sources* 2005;151:18–24. <https://doi.org/10.1016/j.jpowsour.2005.02.048>.
- [6] Xiong Z, Liao S, Dang D, Tian X, Hou S, Liu F, Peng H, Fu Z. Enhanced water management in the cathode of an air-breathing pemfc using a dual catalyst layer and optimizing the gas diffusion and microporous layers. *Int J Hydrogen Energy* 2015;40:3961–7. <https://doi.org/10.1016/j.ijhydene.2015.01.091>.
- [7] Fischer A, Jindra J, Wendt H. Porosity and catalyst utilization of thin layer cathodes in air operated pem-fuel cells. *J Appl Electrochem* 1998;28:277–82. <https://doi.org/10.1023/A:1003259531775>.
- [8] Lee S, Mukerjee S, McBreen J, Rho Y, Kho Y, Lee T. Effects of nafion impregnation on performance of pemfc electrodes. *Electrochim Acta* 1998;43:3693–701. [https://doi.org/10.1016/S0013-4686\(98\)00127-3](https://doi.org/10.1016/S0013-4686(98)00127-3).
- [9] Passalacqua E, Lufrano F, Squadrito G, Patti A, Giorgi L. Nafion content in the catalyst layer of polymer electrolyte fuel cell: effect on the structure and performance. *Electrochim Acta* 2001;46:799–805. [https://doi.org/10.1016/S0013-4686\(00\)00679-4](https://doi.org/10.1016/S0013-4686(00)00679-4).
- [10] Varea A, Monereo O, Xuriguera E, Prades J, Cirera A. Electro spray as a suitable technique for manufacturing carbon-based devices. *J Phys D-Appl Phys* 2017;50:315301–11. <https://doi.org/10.1088/1361-6463/aa798b>.
- [11] Shan N, Jund H, Ahn J, Kim J, Kim S. Electro spray assisted fabrication of porous platinum carbon composite thin layers for enhancing the electrochemical performance of proton exchange membrane fuel cells. *Curr Appl Phys* 2018;18:728–36. <https://doi.org/10.1016/j.cap.2018.01.020>.
- [12] Bodnar E, Grifoll J, Rosell-Llompar J. Polymer solution electro spraying: a tool for engineering particles and films with controlled morphology. *J Aerosol Sci* 2018;125:93–118. <https://doi.org/10.1016/j.jaerosci.2018.04.012>.
- [13] Castillo J, Martin S, Rodriguez-Perez D, Higuera F, Garcia-Ybarra P. Nanostructured porous coating via electro spray atomization and deposition of nanoparticle suspensions. *J Aerosol Sci* 2018;125:148–63. <https://doi.org/10.1016/j.jaerosci.2018.03.004>.
- [14] Yan J, Leng Y, Guo Y, Wang G, Gong H, Guo P, Tan P, Long Y, Liu X, Han W. Highly conductive graphene paper with vertically aligned reduces graphene oxide sheets fabricated by improved electro spray deposition technique. *ACS Appl Mater Interfaces* 2019;11:10810–7. <https://doi.org/10.1021/acsami.8b19811>.
- [15] Chaparro A, Folgado M, Ferreira-Aparicio P, Alonso-Álvarez AMI, Daza L. Properties of catalyst layers for pemfc electrodes prepared by electro spray deposition. *J Electrochem Soc* 2010;157:B993–9. <https://doi.org/10.1149/1.3425740>.
- [16] Chaparro A, Ferreira-Aparicio P, Folgado M, Brightman E, Hinds G. Study of superhydrophobic electro sprayed catalyst layers using a localized reference electrode technique. *J Power Sources* 2016;325:609–19. <https://doi.org/10.1016/j.jpowsour.2016.06.077>.
- [17] Huang Z, Su A, Hsu C, Liu Y. A high-efficiency, compact design of open-cathode type pemfcs with a hydrogen generation system. *Fuel* 2014;122:76–81. <https://doi.org/10.1016/j.fuel.2013.12.058>.
- [18] Wu B, Li B, Liu W, Liu J, Zhao M, Yao Y, Gu J, Zou Z. The performance improvement of membrane and electrode assembly in open-cathode proton exchange membrane fuel cell. *Int J Hydrogen Energy* 2013;10978–84. <https://doi.org/10.1016/j.ijhydene.2013.01.149>. 2013.
- [19] Atkinson R, Rodgers J, Hazard M, Stroman R, Gould B. Influence of cathode gas diffusion media porosity on open-cathode fuel cells. *J Electrochem Soc* 2018;165:F1002–11. <https://doi.org/10.1016/j.jpowsour.2004.01.030>.
- [20] Wang H, Sun N, Zhang L, Zhou R, Ning X, Zhuang X, Long Y, Cheng B. Ordered proton channels constructed from deoxyribonucleic acid-functionalized graphene oxide for proton exchange membranes via electrostatic layer-by-layer deposition. *Int J Hydrogen Energy* 2020;45:27772–8. <https://doi.org/10.1016/j.ijhydene.2020.07.105>.
- [21] Orturk A, Ozcelik N, Yurtcan A. Platinum/graphene nanoplatelets/silicone rubber composites as polymer electrolyte membrane fuel cell catalysts. *Mater Chem Phys* 2021;260:124110. <https://doi.org/10.1016/j.matchemphys.2020.124110>.

- [22] Shai A, Dwivedi C, Manjare S, Kulshrestha V. Sulphonated (pvdf-co-hfp)-graphene oxide composite polymer electrolyte membrane for hi decomposition by electrolysis in thermochemical iodine-sulphur cycle for hydrogen production. *Int J Hydrogen Energy* 2021;46:8852–63. <https://doi.org/10.1016/j.ijhydene.2021.01.027>.
- [23] Fang F, Liu L, Min L, Xu L, Zhang W, Wang Y. Enhanced proton conductivity of nafion membrane with electrically aligned sulfonated graphene nanoplates. *Int J Hydrogen Energy* 2021;46:177784–217792. <https://doi.org/10.1016/j.ijhydene.2021.02.190>.
- [24] Rath R, Kumar P, Rana D, Mishra V, Kumar A, Mohanty S, Nayak S. Sulfonated pvdf nanocomposite membranes tailored with graphene oxide nanoparticles: improved proton conductivity and membrane selectivity thereof. *J Math Sci* 2022;57:3565–85. <https://doi.org/10.1007/s10853-021-06803-3>.
- [25] Wu J, Yi B, Hou M, Hou Z, Zhang H. Influence of catalyst layer structure on the current distribution of pemfcs. *Electrochim Solid State Lett* 2004;6:151–4. <https://doi.org/10.1016/j.electacta.2021.138793>.
- [26] Huang H, Guo Z, Yang P, Chen P, Wu J. Electrical conductivity and hydrophobicity of graphene oxide-modified carbon nanofibers. *Chem Phys Lett* 2021;771:138551–60. <https://doi.org/10.1016/j.cplett.2021.138551>.
- [27] Shahryari Z, Yeganeh M, Gheisari K, Ramezanzadeh B. A brief review of the graphene oxide-based polymer nanocomposite coatings: preparation, characterization and properties. *J Coating Technol Res* 2021. <https://doi.org/10.1007/s11998-021-00488-8>.
- [28] Obeisun O, Meyer Q, Robinson J, Gibbs C, Kucernak A, Shearing P, Brett D. Development of open-cathode polymer electrolyte fuel cells using printed circuit board flow-field plates: flow geometry characterization. *Int J Hydrogen Energy* 2014;39:18326–36. <https://doi.org/10.1016/j.ijhydene.2014.08.106>.
- [29] Navarro AJ, Gómez MA, Daza L, Molina-García A, López-Cascales JJ. Influence of the gas diffusion layer on the performance of an open cathode polymer electrolyte membrane fuel cell. *Int J Hydrogen Energy* 2022;47:7990–9. <https://doi.org/10.1016/j.ijhydene.2021.12.151>.
- [30] Kim J, Lee S, Srinivasan S. Modeling of proton exchange membrane fuel cell performance with an empirical equation. *J Electrochem Soc* 1995;142:2670–4. <https://doi.org/10.1149/1.2050072>.
- [31] Liu X, Peng F, Lou G, Wen Z. Liquid water transport characteristics of porous diffusion media in polymer electrolyte membrane fuel cells: a review. *J Power Sources* 2015;299:85–96. <https://doi.org/10.1016/j.jpowsour.2015.08.092>.
- [32] Cassie A, Baxter S. Wettability of porous surfaces. *Trans Faraday Soc* 1944;40:546–51. <https://doi.org/10.1039/TF9444000546>.
- [33] Lapique F, Belhadj M, Bonnet C, Pauchet J, Thomas Y. A critical review on gas diffusion micro and macroporous layers degradations for improved membrane fuel cell durability. *J Power Sources* 2016;336:40–53. <https://doi.org/10.1016/j.jpowsour.2016.10.037>.
- [34] Miccoli I, Edler F, Pfnür H, Tegenkamp C. The 100th anniversary of the four-point probe technique: the role of probe geometries in isotropic and anisotropic systems. *J Phys-Condens Matter* 2015;27:223201–30. <https://doi.org/10.1088/0953-8984/27/22/223201>.
- [35] Alarifi I. Investigation the conductivity of carbon fiber composites focusing on measurement techniques under dynamic and static loads. *J. Mater. Res. Technol-JMRT* 2019;8:4863–93. <https://doi.org/10.1016/j.jmrt.2019.08.019>.
- [36] Owejan J, Owejan J, Gu W, Trabold T, Tighe tW, Mathias M. Water transport mechanism in pemfc gas diffusion layers. *J Electrochem Soc* 2010;157:B1456–64. <https://doi.org/10.1149/1.3468615>.